Mine Water Environ (2015) 34:417–429
DOI 10.1007/s10230-014-0316-2

TECHNICAL ARTICLE

Metalloid Attenuation from Runoff Waters at an Historic Orogenic Gold Mine, New Zealand

J. Druzbicka · D. Craw

Received: 29 January 2014 / Accepted: 3 November 2014 / Published online: 24 December 2014

Abstract The metalloids arsenic and antimony are mobilised through the decomposition of arsenopyrite, pyrite, and stibnite at the historic Big River Mine. Their content in the solid substrates reach levels up to ≈25 wt% As and 3.6 wt% Sb, but their concentrations in the mine water are only elevated locally, up to 0.85 mg/L dissolved As and 0.007 mg/L dissolved Sb. Water draining the waste rock are characterised by neutral pH, but at the mine's former processing site, the oxidation of sulphide concentrates has produced acidic conditions, both in the water (pH 3.8) and solid mining residues (paste pH 2–4). Dissolved metalloid concentrations are being effectively attenuated on site through the formation of secondary As phases in the mining residues, including scorodite, iron sulphoarsenate, and amorphous iron arsenate. Attenuation is also occurring by co-precipitation and adsorption onto iron oxides or hydroxides, and adsorption onto clay mineral surfaces. These processes are complemented by dilution of the dissolved As and Sb by the Big River. Therefore, despite the extremely high levels of As and Sb in the mining residues, metalloid mobilisation is limited, resulting in relatively low concentrations in water leaving the site.

Keywords Gold mining · Arsenic · Antimony · Metalloid mobility · Mining residues

Introduction

The mining legacy from orogenic gold deposits commonly involves elevated arsenic (As) and antimony (Sb) concentrations in water as well as soils and remaining mining wastes because of the natural, close geochemical relationship between gold and the two metalloids, and the fact that mining and beneficiation of deposits facilitate mobilisation of these metalloids (Ashley et al. 2003; Groves et al. 1998; Haffert et al. 2010; Lottermoser 2010). Both As and Sb are found in sulphide minerals in orogenic vein systems and are typically present at levels of hundreds to thousands of times above typical crustal abundance values (Craw et al. 2004). The presence of elevated As and Sb concentrations in water and soil is an issue of environmental concern, as both metalloids are considered toxic or potentially toxic at low levels (e.g. <0.01 mg/L in water).

Metalloid concentrations in mine waters of the South Island of New Zealand are in some cases known to reach extreme levels, such as the 52 mg/L As at the historic Blackwater Mine (Haffert and Craw 2008a). In this paper, we present an example of the historic Big River Mine where metalloid concentrations in mine waters are minor, despite some very high concentrations of As and Sb at the site, and despite the site being under the influence of the same wet climatic conditions as the Blackwater Mine mentioned above. The purpose of this study was to quantify the metalloid concentrations in the mine water and solid residues, and to investigate the mechanisms of As and Sb attenuation at the Big River Mine. These results are potentially relevant to other abandoned and active orogenic gold mines with elevated As and Sb around the world.

General Setting

Basement rocks in the Big River Mine area belong to the Paleozoic Greenland Group, and comprise alternating

J. Druzbicka (✉) · D. Craw
Geology Department, University of Otago,
PO Box 56, Dunedin 9054, New Zealand
e-mail: joanna.druz@gmail.com

sequences of weakly metamorphosed greywackes and argillites (Christie et al. 2000; Cooper 1974; Laird and Shelley 1974). The rocks have high acid neutralizing capacity (ANC), typically ranging from 4 to 9 wt% $CaCO_3$ equivalent (Hewlett et al. 2005). The high ANC generally exceeds the maximum potential acidity (MPA) of the Greenland Group rocks (Haffert et al. 2006). Mesozoic granitoids are faulted against the eastern margin of the Greenland Group rocks (Barry and Armstrong 1993; Tulloch 1983), and Reefton Group rocks (quartzite, mudstone, and impure limestone) lie unconformably on top of the Greenland Group rocks directly to the east and within the Big River mining area (Barry and Armstrong 1993; Gage 1948). The Big River deposit is situated within the overturned eastern fold limb of a regional syncline, and the associated intensely deformed nature of the ore bodies was a hindrance during mining (Barry and Armstrong 1993; Gage 1948).

Gold in the orogenic Reefton goldfield, of which the Big River deposit is part, occurs in free form (minor) as well as in association with sulphide minerals (pyrite, arsenopyrite, and stibnite) in shear zone-hosted quartz veins (Christie et al. 2010). Gold is also present in sulphide-rich fault gouge zones as well as in disseminated sulphides in the surrounding host rocks (Barry and Armstrong 1993; Christie and Brathwaite 2003; Milham and Craw 2009).

Big River Site

The Big River site lies at an elevation of 700–800 m above sea level (asl), and is drained by the Big River, which originates from the hills to the east of the site and joins Grey River to the west. The Big River is characterised by deeply orange-brown colour of the water. This is likely due to the presence of humic substances, which is typical of the waterways in the region (Winterbourn and Collier 1987). Two tributaries join Big River in the vicinity of the mine site (Fig. 1a, b). The region is characterised by high orographic rainfall (more than 2,000 mm annually) and the mean annual temperature is 12 °C. The vegetation cover is predominantly composed of a mixed beech (*Nothofagus* spp.) and podocarp forest. The Big River mine produced over 4.2 t of gold between the 1880s and 1942 (Barry and Armstrong 1993; Christie et al. 2000; Henderson 1917). Only the quartz vein hosted mineralisation was targeted during historic mining. As in the case of other nearby historic mines, mining undertaken at the Big River site was unregulated from the environmental control perspective, and the metalloid-rich concentrates and tailings were disposed of on-site or directly into the adjacent Big River (Fig. 1a, b). No remediation efforts have been attempted at the site since its closure in 1942.

Following extraction from the mine, ore was transported to the processing site approx. 1 km away using an aerial ropeway (Fig. 1a). The mined waste rocks were deposited down the sides of the hill that the shaft was driven into as well as on a smaller mullock heap outside of the adit No. 1 entrance (Fig. 1a). Two streams drain the main waste rock pile, on the western and southern side of the hill. The creeks merge further downstream and join the Big River at the battery site within the historic mine processing area (Fig. 1a, b). A small dam has formed at the No. 1 adit entrance (Fig. 1a) and no water emanated from the tunnel at the time of the site visit.

The processing site occupies a clearing alongside the Big River (Fig. 1a, b). Gold extraction involved crushing of the quartz ore in a stamper battery, followed by mercury amalgamation and/or cyanidation. No roasting of the ore was undertaken at the Big River Mine. Instead, ore concentrate was produced, which was then periodically sent overseas for the recovery of the sulphide-enclosed gold (Wright 1993). The battery site is located on the river bank and lies partly on a slope, which during rain events allows the movement of surface runoff waters directly through the site (Fig. 1b). Most of the site remains unvegetated and contains brown/orange mining residues. Crushed ore was stockpiled for further processing at two locations within the processing site: ore heap #1 and #2 (Fig. 1b). These locations still contain some of the original crushed ore, now in the form of orange-coloured sand/clay residues, and are only partly vegetated. The western side of the Big River processing site is not well drained and a number of waterlogged and swampy areas surround the two ore heaps. A cyanide plant was located on the river bank and 7 tanks still remain on site (Fig. 1b). Some of the tanks are half-filled with residues and soil and are mostly covered by vegetation. The land between the tanks is also fully vegetated.

Methods

Sampling

Six water samples were collected from the Big River mining area (Fig. 1b), which included Big River water upstream (BRW1) and downstream (BRW2) of the processing site, ore heap seepage (BRW3), the processing site drain (BRW4), and the stream draining the large mullock heap (BRW5-6) (Fig. 1a, b). Water samples were filtered in situ (0.45 μm) and collected in nitric acid-washed plastic bottles. Flow rates of small seeps (samples BRW3-6) were estimated by timing the collection of the flow into a container of known volume.

Thirty-six solid samples were collected from the processing area of the mine, at the battery site (20), ore heaps

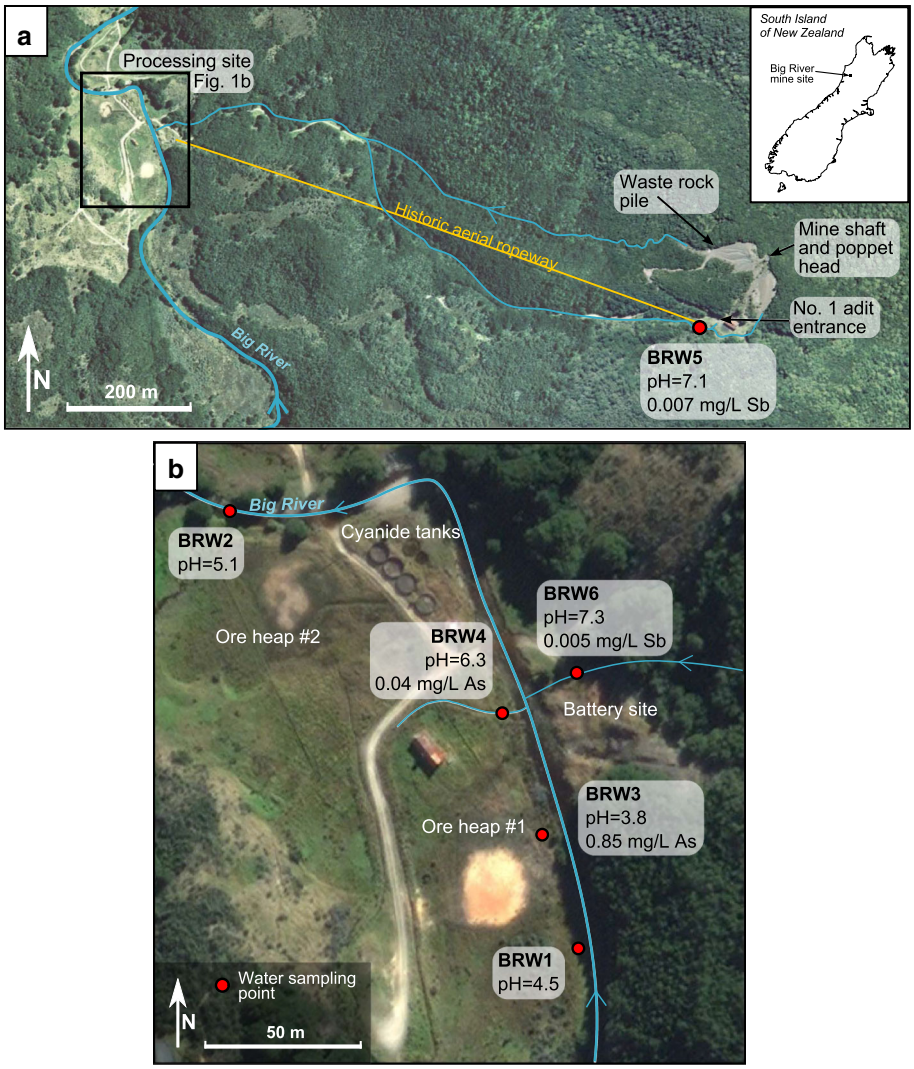

Fig. 1 Aerial photographs showing the Big River mine site, water sampling locations, and analytical results. Only concentrations above minimum detection limits of the metalloids are included. **a** View of the Big River mine showing the location of the mine shaft with surrounding it waste rock pile in relation to the processing site (aerial image provided by OceanaGold Ltd), **b** Close up view of the processing site showing the locations of the battery site, two ore storage areas and the cyanide plant (satellite image from Google Earth)

(14), and cyanide plant mining residues and soils (2). Approximately 200 g of each substrate was collected in clean plastic bags. The samples were used for the determination of paste pH and per cent moisture content and for the correction of field portable X-ray fluorescence (FPXRF) results. In addition, 15 samples were subjected to scanning electron microscopy with energy dispersive spectroscopy (SEM–EDS) and/or X-ray diffraction (XRD). Various substrates representing a wide spectrum of As and Sb contents were collected, based on observations during the preliminary site reconnaissance.

Analytical Methods

The six field-filtered (0.45 µm membrane filter) water samples were analysed for dissolved As and Sb using inductively coupled plasma mass spectrometry (ICP-MS) at Hill Laboratories, an internationally accredited laboratory in Hamilton, NZ. Standard APHA method 3125B was followed and the method's detection limits were 0.02 mg/L for As and 0.004 mg/L for Sb (APHA 2005). Water sampling was accompanied by pH measurements, which were performed using a pre-calibrated Oakton pH 310 series hand-held meter.

Paste pH analyses were performed on 36 sampled mine residues in the laboratory using the same pH meter. The method followed was that outlined by Blakemore et al. (1987). Approximately 20 g of each sample material was air dried and sieved below 2 mm. Mixtures of sample materials and distilled water were prepared according to the recommended 1:2.5 weight ratio (10 g of material was mixed with 25 mL of water). The mixtures were vigorously stirred with a glass rod, left overnight, and analysed the following morning. Three readings were recorded for each sample and a mean was calculated and used as the final result.

An Innov-X Systems Alpha Series™ model A-6500 FPXRF was used for delineation of the metalloid contents

at the mine's processing site. US-EPA (2007) method 6200 guidelines were followed and all analyses were performed in soil mode over ≈30 s acquisition time. The As and Sb detection limits of the FPXRF method, which were displayed with each analysis, were typically approx. 30 mg/kg for As and 60 mg/kg for Sb. Field analyses were performed on a grid that ranged from 2 × 2 m, through 3 × 3 m to 4 × 4 m, depending on the location surveyed. The extent and distribution of the performed analyses was governed by the accessibility of the substrates, which mainly depended on the presence of thick vegetation and/or waterlogged ground conditions. Very similar in situ FPXRF arsenic analyses were performed by Haffert and Craw (2009) at the nearby Blackwater mine site, using the same FPXRF unit. The FPXRF results obtained then were found to correlate well with the laboratory ICP-MS analyses performed on the same materials (Haffert and Craw 2009). The FPXRF data was also found to be adequately precise (RSD <20 %; Haffert and Craw 2009; US-EPA 2007), with the level of precision rising with the level of metalloid content (Haffert and Craw 2009).

Moisture content of the Big River substrates ranged from <1 to 76 % total weight (mean = 10 %), with the highest results obtained from fine-grained and clay-rich substrates (Table 1). It was anticipated that high moisture content may have been a source of error during the FPXRF analyses, particularly in samples with moisture levels exceeding 20 % (US-EPA 2007). However, in this case, moisture-related error can be dismissed as relatively insignificant because of the very high metalloid contents involved (wt% levels), and also because of the purpose of the study, which merely requires semi-quantitative analyses for mapping of relative metalloid contents. The theoretically possible element interference between As and lead in FPXRF analyses was dismissed as a source of error for the FPXRF analyses as at no point was the Pb:As concentration ratios found to be close to the 10:1 ratio which, according to US-EPA (2007), is the ratio at which or above such interference may occur.

The 36 solid samples collected were subjected to laboratory XRF analyses for As, Sb, and Pb. The analyses were performed by SpectraChem Analytical, an IANZ certified laboratory in Lower Hutt, New Zealand. Initial sample preparation included air drying and milling to <100 μm with a TEMA mill. The samples were then dried at 110 °C and pressed-powder discs (30 mm in diameter) were prepared using 10 % Merck Hoechst wax C micropowder. The analyses were performed using a Siemens/Bruker SRS303AS wavelength-dispersive X-Ray spectrometer fitted with a 3 kW generator. The metalloid detection limits were 20 mg/kg. Internationally-certified and laboratory-manufactured standards were used to calibrate the instrument, including five USGS-manufactured certified reference materials (GXR-1–GXR-4 and GXR-6), which were used as As (As from 25 to 3.970 mg/kg) and Pb standards, one internationally certified "glass standard" ANRT VS-N used for Sb (800 mg/kg), as well as three laboratory-prepared standards manufactured from stibnite and sand mixtures (ranging from 0.5 to 5 wt% Sb). The FPXRF As and Sb results on the 36 samples were plotted against the results obtained with the laboratory XRF. This comparison provided an equation of the best fit line, which was used for the correction of the FPXRF results from the field. The corrected data were then used to map the metalloid contents.

Fifteen out of the 36 samples were selected for the XRD analyses, including materials from four processing areas at the site (Fig. 1a, b). The samples were air dried for 7 days and milled to <100 μm using a TEMA mill with tungsten carbide container and rings. Samples were then placed in sample holders and analysed using a PANalytical X'Pert-Pro MPD PW3040/60 (Philips, The Netherlands) with Cu Kα radiation at the Geology Dept., University of Otago. The powder diffraction patterns were analysed with the PANalytical High Score software package.

The SEM–EDS imaging and analyses were performed using a Zeiss Sigma variable pressure field emission gun (VP FEG) SEM fitted with the HKL INCA Premium Synergy Integrated ED/EBSD system (Oxford Instruments, Oxfordshire, UK) operated at 15 kV, at the Otago Centre for Electron Microscopy (OCEM) at the University of Otago. EDS was used for qualitative and quantitative analyses, which included the production of elemental distribution maps, of two sample materials (B-1 and B-2) prepared as polished sections.

Results

Site Chemistry

The six water samples collected from the surrounding creeks, seepage areas, and the Big River ranged in pH from 3.8 (ore heap #1 seepage) to 7.3 (creek draining waste rock pile) (Fig. 1b). The As and Sb concentrations were typically below the detection limits of the methods used (0.02 mg/L for As and 0.004 mg/L for Sb). The highest As concentration, 0.85 mg/L, was recorded in the ore heap #1 seepage, while the highest Sb concentration, 0.007 mg/L, was recorded in the creek draining the waste rock pile (Fig. 1a, b). Both As and Sb were undetectable in Big River water, where the measured pH was close to 5 (Fig. 1b).

Mining-related processing residues are found in four areas around the Big River mine processing site: the battery site, two ore storage areas (i.e. ore heap #1 and 2), and the cyanide plant. Sample descriptions and analytical results for materials

Table 1 Descriptions and analytical results of 36 sampled mining residues

ID	Description	Paste pH	% moisture	As (mg/kg)	Sb (mg/kg)	Mineralogy (XRD)
B-1	Fully cemented residue (hardpan) (Gn/Bn)	1.80	4.1	132,000	19,218	Qtz, py, scor, musc, aspy
B-2	Partially cemented residue (Y)	2.44	24.2	162,100	10,371	Qtz, bukovskyite (?)
B-3	Fine-grained residue (Y)	2.81	76.2	231,300	35,606	Amorphous+qtz
B-4	Fine-grained substrate (G)	1.75	7.1	26,410	355	Qtz, musc, aspy
B-5	Poorly-sorted residue (Bn)	3.21	4.3	18,060	1,662	
B-6	Well-sorted fine-grained sand (Bn)	3.10	7.3	25,850	4,767	Qtz, musc, kaol
B-7	Medium-grained sand, some cemented (Gn)	2.40	17.8	69,070	6,750	
B-8	Poorly-sorted residue (Bn)	2.76	9.5	112,900	20,376	Qtz, musc
B-9	Fine to medium-grained sand, partially cemented (Bn)	2.36	11.8	102,900	6,842	
B-10	Mine soil (Bn)	3.16	8.5	33,050	2,601	
B-11	Fine-grained residue (Bn)	2.64	26.0	71,900	27,928	Qtz, musc, kaol
B-12	Fine-grained residue (Y)	2.82	34.2	147,500	22,416	Qtz, musc
B-13	Fine to medium-grained sand (O)	3.43	4.3	8,960	333	Qtz, musc, kaol
B-14	Fine to medium-grained sand (Bn)	2.88	5.9	54,960	9,638	
B-15	Medium-grained sand (Bn/G)	2.20	7.3	16,920	851	
B-16	Medium-grained sand (Bn)	2.81	7.1	62,860	11,804	Qtz, musc, kaol
B-17	Fine to medium-grained sand (O/Bn)	3.18	5.2	2,200	691	
B-18	Well-sorted medium-grained sand (G/Bn)	2.70	8.6	9,020	994	
B-19	Fine-grained substrate (G)	1.60	14.6	34,640	298	
B-20	Fine-grained substrate (G)	2.28	4.3	21,310	411	
OH1-1	Well-sorted medium-grained sand (O)	3.50	1.0	3,850	138	Qtz, musc, kaol
OH1-2	Well-sorted medium-grained sand (O)	3.45	1.2	4,340	315	
OH1-3	Well-sorted medium-grained sand (O)	3.51	1.2	4,320	206	Qtz, musc, kaol
OH1-4	Well-sorted medium-grained sand (O)	3.43	1.2	3,060	93	
OH1-5	Well-sorted medium-grained sand (O)	3.65	1.5	3,960	60	
OH1-6	Well-sorted medium-grained sand (O)	3.64	1.2	4,210	91	
OH1-7	Well-sorted medium-grained sand (O)	3.60	8.0	1,570	<MDL	
OH1-8	Well-sorted medium-grained sand (O)	3.78	1.1	3,840	172	
OH1-9	Well-sorted medium-grained sand (O)	3.27	13.3	2,080	76	
OH1-10	Well-sorted medium-grained sand (O)	3.77	1.4	6,350	160	
OH1-11	Well-sorted medium-grained sand (O)	3.51	11.9	514	39	
OH2-1	Clay-rich residue (O)	5.35	16.3	3,460	1,226	Qtz, musc, kaol
OH2-2	Clay-rich residue (O)	5.83	10.7	2,850	1,983	Qtz, musc, kaol
OH2-3	Clay-rich residue (O)	5.80	6.4	2,440	770	
CT-1	Mine soil (Bn)	6.20	3.4	2,290	435	Qtz, musc, kaol
CT-2	Mine soil (Bn)	3.97	3.1	2,660	218	

Sample IDs correspond to the area where the materials were obtained from, with B representing battery site, OH1-ore heap #1, OH2-ore heap #2, and CT-cyanide tanks. The arsenic and antimony analytical results were obtained with a laboratory-based XRF method

Bn brown, *G* grey, *Gn* green, *O* orange, *Y* yellow, *MDL* minimum detection limit, *aspy* arsenopyrite, *kaol* kaolinite, *musc* muscovite, *py* pyrite, *qtz* quartz, *scor* scorodite

derived from these four areas are presented in Table 1. The paste pH measurements of the 36 substrates show that all are acidic (Table 1). The average pH results for the different areas were 5.6 at the ore heap #2, 4.3 at the cyanide tanks, 3.5 at the ore heap #1, and 2.3 at the battery site.

Maps in Fig. 2a, b show As and Sb content (corrected values) recorded at the mine's processing site. By far, the highest As and Sb concentrations were encountered at the battery site, where they reached up to 25 and 2.8 wt%, respectively (Table 1; Fig. 2a, b). These high results were concentrated in two distinct areas of the battery site (Fig. 2a, b). Metalloid contents of the two ore heaps and the cyanide tank areas were generally below 1 wt% in the case of As and below 0.5 wt% in the case of Sb. Higher As

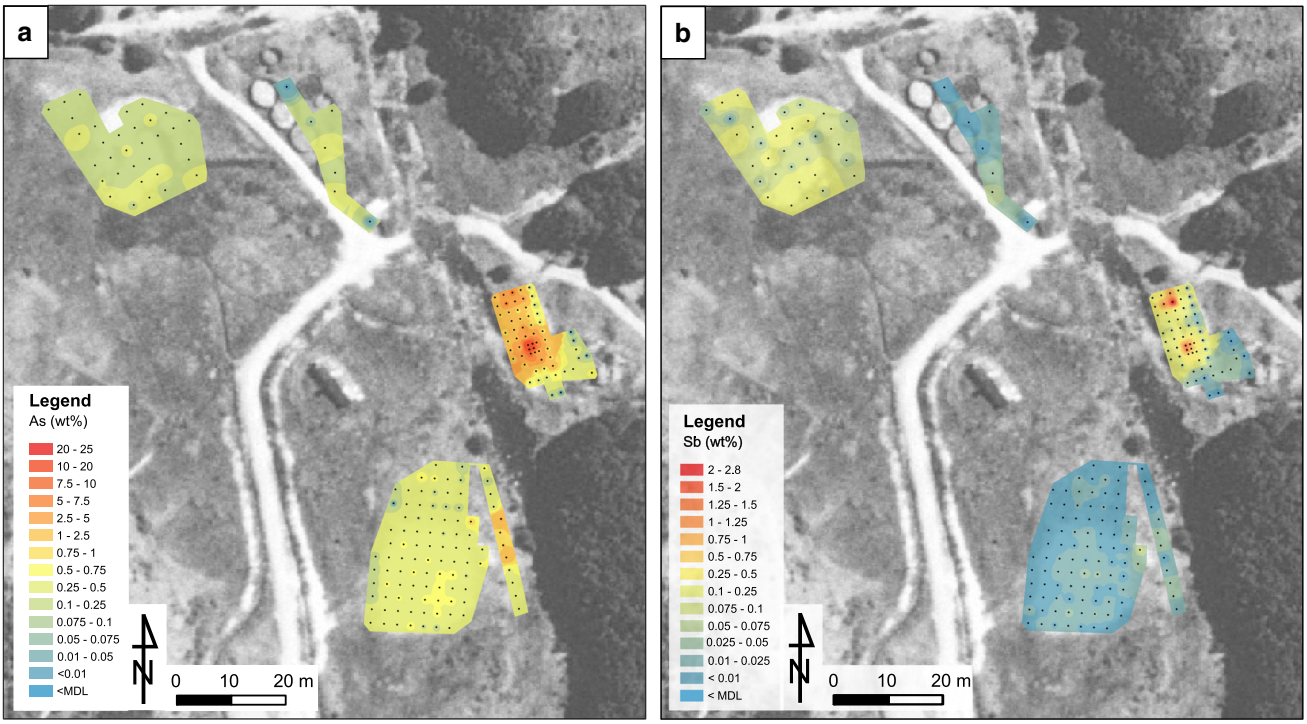

Fig. 2 Arsenic (**a**) and antimony (**b**) distribution in four areas of the Big River mine's processing site based on corrected results of the FPXRF analyses

content, reaching up to 2.6 wt%, were recorded on the side of the ore heap #1 (Fig. 2a), directly in the vicinity of Big River, in an area where the heap drains during wet periods.

Mineralogy of Battery Site Wastes

The most prominent feature of the battery site (Fig. 1b) is a relict timber structure, approximately square in shape and 2 m by 2 m in size. The structure, together with its associated well-cemented mining residues, forms an unvegetated mound approximately 2 m above the Big River's water level. The residues form a hardpan that extends down the $\approx$1 m slope. In hand specimen (sample B-1, Table 1), the substrate is predominantly green–brown in colour and quartz as well as pyrite/arsenopyrite grains are visible to the naked eye. XRF analysis of the material indicated 13.2 wt% As and 1.9 wt% Sb; XRD results indicated the presence of quartz, scorodite, arsenopyrite, pyrite, and muscovite (Table 1). The presence of these minerals, as well as an additional phase that has not been identified using XRD, was also confirmed petrographically (Fig. 3a, b). Arsenopyrite and minor pyrite grains have undergone varying degrees of partial decomposition. Some grains appear to retain much of their euhedral shape (right side of image in Fig. 3b), while other grains have serrated edges (centre top, arrowed) or appear as a collection of small (<30 μm) shards (left side of image, arrowed). The interstitial space between quartz and primary sulphide minerals is filled with two clearly distinguishable phases, of which one (scorodite, $FeAsO_4{\cdot}2H_2O$) is pale green–grey and the other is orange in plane polarised light (PPA) (Fig. 3a). Backscatter electron (BSE) images and element maps of sample B-1 (Figs. 4, 5) show the partial decomposition of arsenopyrite (Fig. 4) and stibnite (Fig. 5) grains and the cementing nature of the surrounding As–(Sb)–Fe phases. The phases can be seen coating sulphide minerals as well as the nearby angular to subangular quartz grains (Figs. 4, 5).

Ten point analyses (S1–S10) as well as one line analysis were performed to further quantify the detailed variations in metalloid mineralogy in the cemented material (Figs. 4, 6a–e). These data distinguish between scorodite and two other As–Fe phases, one of which is characterised by high Sb content and the other by the presence of sulphur. Scorodite is seen as a slightly darker shade of grey and globular-looking material and appears to be often enclosed within the other, light grey, As–Sb–Fe phase (e.g. Fig. 6a). Scorodite, represented by the point analyses numbered S1–S5, contains impurities of Sb and S of <3 wt% and ≤1 wt%, respectively, and was identified around the decomposing arsenopyrite and stibnite minerals (Figs. 4, 6a, b). The globular nature of scorodite and its relationship with the other, As–Sb–Fe, phase is particularly visible in Fig. 6a. The corresponding line analysis results, shown in

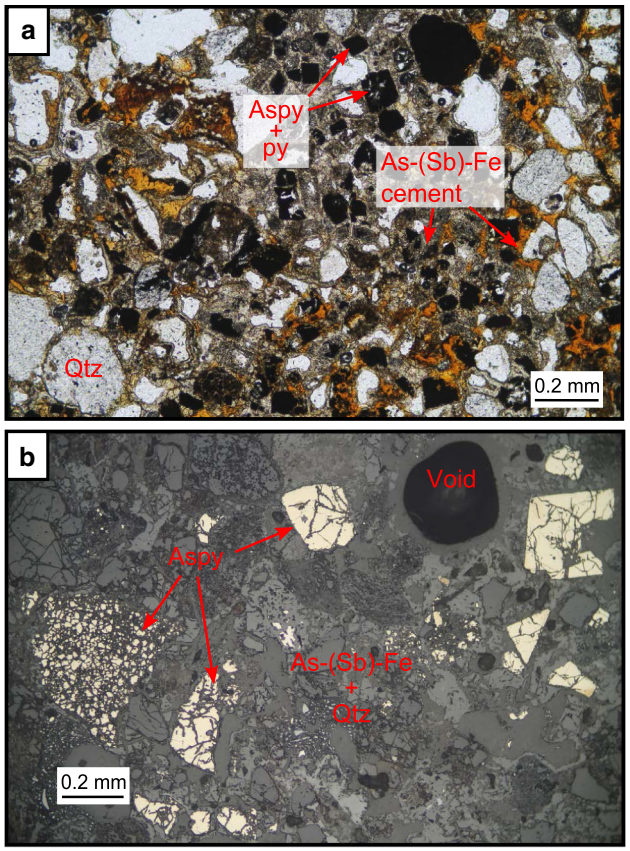

Fig. 3 **a** Microscope image of sample B-1 under plane-polarised light (PPL) showing abundant sulphide minerals (opaque) as well as *pale green* and *orange* cement. **b** Reflected light microscope (REF) image of the same sample showing arsenopyrite grains at different stages of decomposition

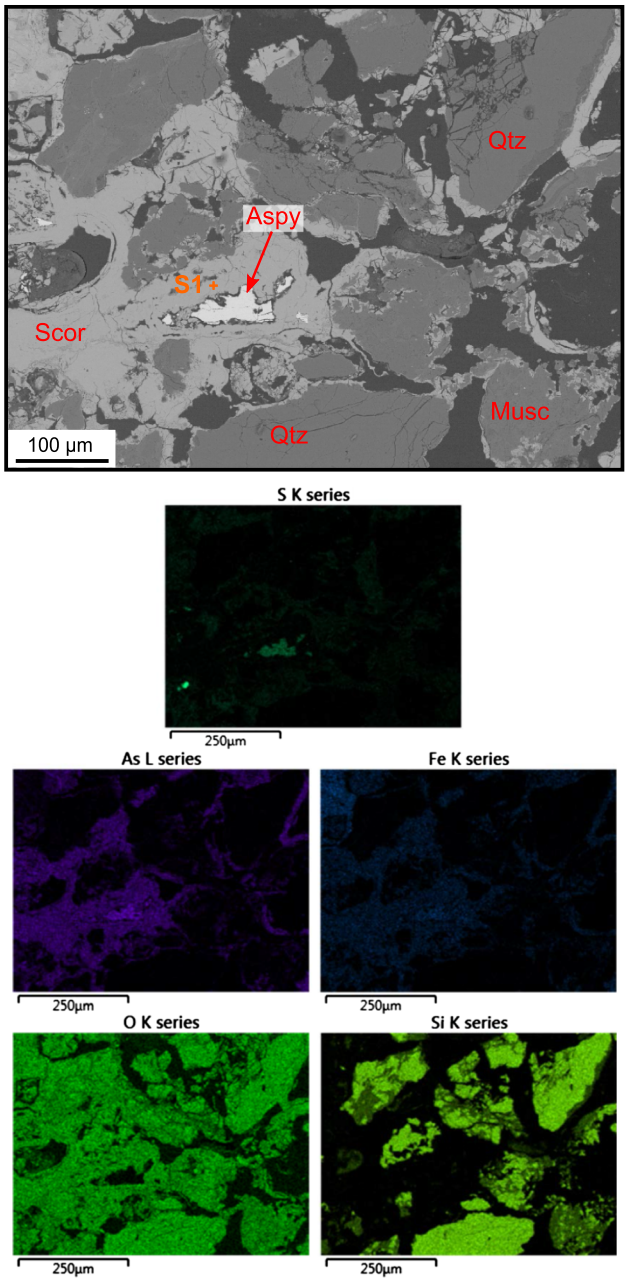

Fig. 4 Backscatter electron (BSE) image of sample B-1 showing decomposing arsenopyrite grain and the cementing nature of scorodite, with corresponding S, As, Fe, O, and Si element maps. The brighter the *colour* on the element maps, the higher the concentration. Location of EDS spot analysis (*S1*) is also indicated

Fig. 6d, illustrate the higher As, Fe, O, and considerably lower Sb and S concentrations in scorodite, relative to the immediately surrounding it phase. The mineral located in the immediate vicinity of the stibnite grains in Fig. 6a and b is an As–Sb–Fe phase, in which both As and Sb contents range between ≈15 and 35 wt% (Fig. 6d and point analyses S6–S8 in Fig. 6e). Point analyses S9 and S10 were performed on the interstitial material surrounding an arsenian pyrite grain (Fig. 6c). This phase was found to contain sulphur (≈6 wt%), as well as 26 wt% As, 24 wt% Fe, and 3 wt% Sb (Fig. 6c, e).

Distinctive, creamy-yellow coloured residues were also found beside the timber structure at the battery site (sample B-2, Table 1). The XRF analysis of this material indicates As and Sb contents of approximately 16 and 1 wt%, respectively (Table 1). In hand specimen, the material ranges from fine-grained clay-like loose material to more consolidated fragments forming aggregates on a centimetre scale. The microscope image taken under PPL presented in Fig. 7a indicates that, apart from sub-rounded quartz grains (arrowed, on average 0.1–0.2 mm in size), there are two phases present. One of them appears bright orange while the other is dark brown (Fig. 7a). The brown-coloured phase tends to be present around the outer edges of the first mineral, forming a rim, and the boundary between the two is uneven. The brown phase also acts as cement and can be seen coating the quartz grains present (Fig. 7a).

Energy dispersive spectroscopy analyses of the two phases revealed differences in their composition. On the

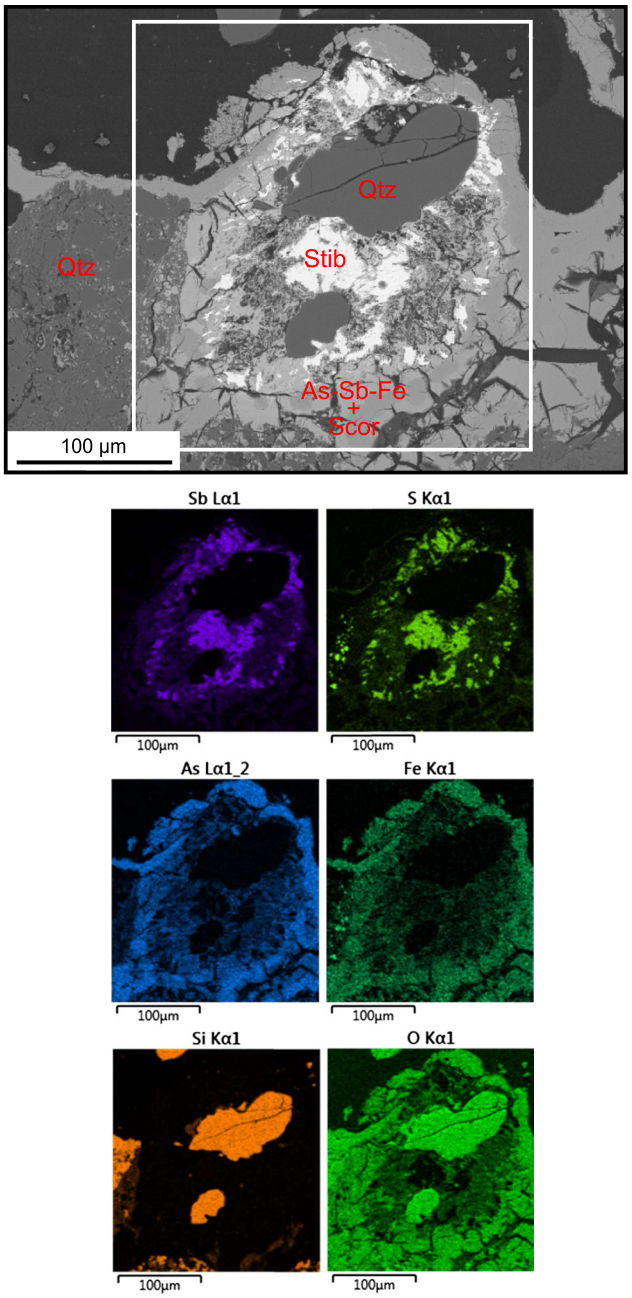

Fig. 5 Backscatter electron (BSE) image of sample B-1 showing decomposing stibnite grain and the surrounding cementing phases (As–Sb–Fe and scorodite), as well as corresponding Sb, S, As, Fe, Si, and O element maps. The extent of the element maps' view is marked with a *white rectangle* on the BSE image. The brighter the *colour* on the element maps, the higher the concentration

BSE image, the dominant grey phase (orange under PPL) contained ≈30 wt% Fe, 22 wt% As, and 8 wt% S (Fig. 7b). The light grey mineral on the other hand (dark brown under PPL, Fig. 7a) contained a higher proportion of arsenic (27 wt%) as well as some antimony (1.5 wt%), while the iron content remained at 30 wt% (Fig. 7b). Unlike sample B-1, no residual sulphide minerals were found in sample B-2. XRD analysis of the material failed to identify any known iron arsenate or iron (hydr)oxide phases (Table 1). The closest, although not perfect, match found was an iron arsenate sulphate mineral, bukovskyite ($Fe_2[AsO_4][SO_4][OH]\cdot 7H_2O$). However, the relative molar proportions of the elements present, as recorded by the EDS analyses, did not agree with the known bukovskyite composition (52.3 % O, 22.8 % Fe, 15.3 % As, 6.6 % S).

A bright yellow substrate sampled from the battery site (sample B-3, Table 1) was a clay-like powdery material found to contain some of the highest metalloid contents recorded at the Big River mine site: 23 wt% As and 3.6 wt% Sb. The XRD pattern was characterized by high background intensities and no clear peaks (except for quartz), indicative of a highly disordered (amorphous) material (Table 1).

Sample B-4, collected from an area near the Big River's water edge at the battery site, was a fine-grained distinctly grey-coloured material containing visible quartz sand grains. XRD analysis revealed the presence of arsenopyrite in this substrate (Table 1).

Discussion

Metalloid Mobility and Attenuation in Mining Residues

Indirectly, metalloids mobility is controlled by the environmental conditions present on site, in particular the pH, which governs the precipitation and dissolution of the secondary phases present. For instance, the low pH levels present at the battery site enable the sustained presence of scorodite, since the mineral is relatively stable in acidic conditions and redissolves at pH 7–8 (Krause and Ettel 1989; Langmuir et al. 2006). The presence and continued survival of scorodite contributes to the minimisation of arsenic mobility at the Big River battery site. The formation of secondary As minerals such as scorodite, is one of the mechanisms of As retention in sulphidic mining wastes (Ashley and Lottermoser 1999; DeSisto et al. 2011; Filippi et al. 2009; Foster et al. 1998; Frau and Ardau 2004; Gieré et al. 2003; Haffert et al. 2010; Salzsauler et al. 2005). Some of the highest As and Sb contents recorded at the Big River battery site were associated with arsenopyrite-rich hardpan material containing scorodite (sample B-1), as well as suspected amorphous iron arsenate (sample B-3, ≈23 wt% As and 3.6 wt% Sb) and iron sulphoarsenate (sample B-2, ≈16 wt% As and 1 wt% Sb) (Table 1). Comparisons with historic photographs of the site indicated that the two areas where samples B-1 to B-3 were collected from, which have the highest metalloid contents (Fig. 2a, b), were the locations of an intermediate concentrate holding area and a concentrates shed. Metalloid mobilisation occurred on a

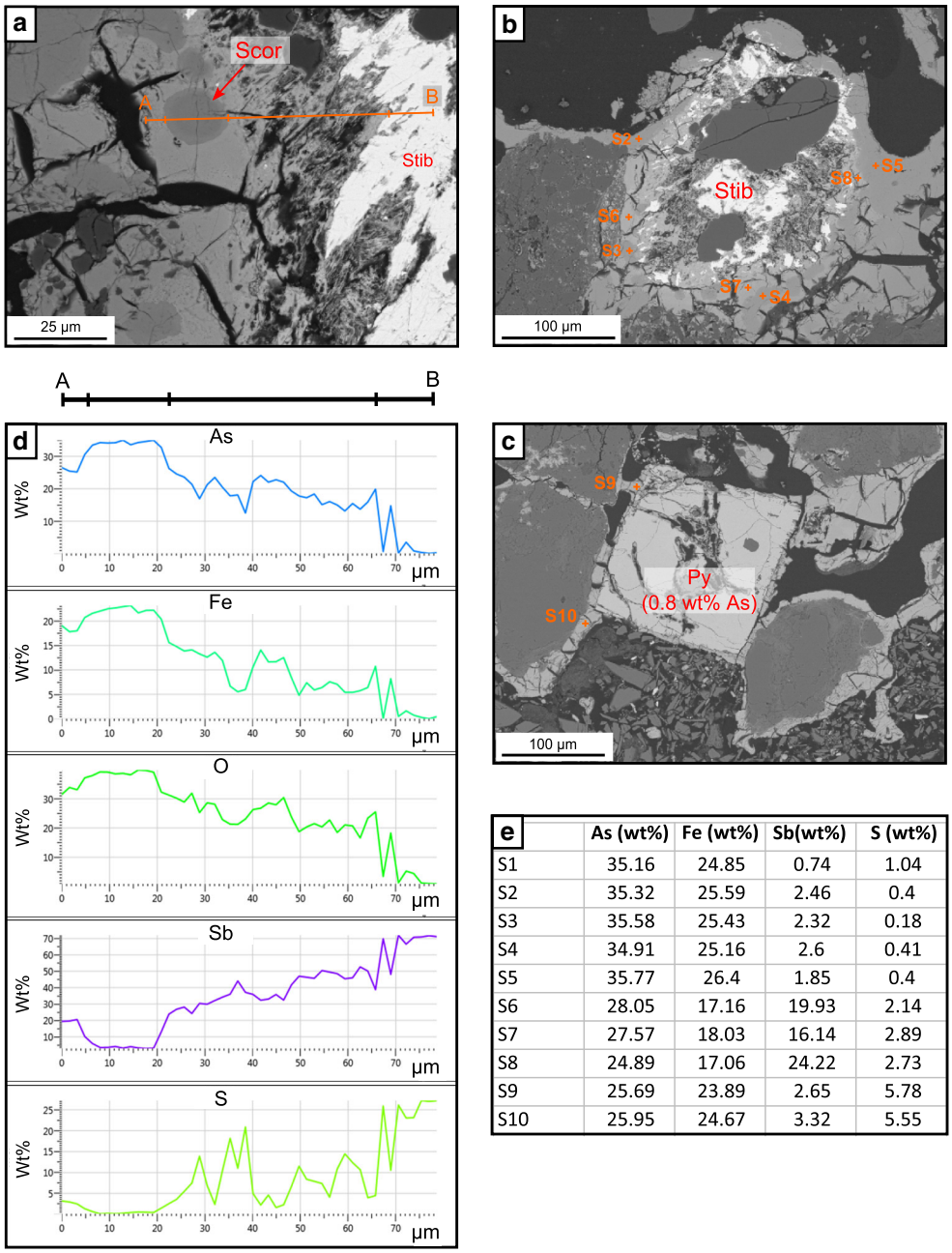

e

	As (wt%)	Fe (wt%)	Sb(wt%)	S (wt%)
S1	35.16	24.85	0.74	1.04
S2	35.32	25.59	2.46	0.4
S3	35.58	25.43	2.32	0.18
S4	34.91	25.16	2.6	0.41
S5	35.77	26.4	1.85	0.4
S6	28.05	17.16	19.93	2.14
S7	27.57	18.03	16.14	2.89
S8	24.89	17.06	24.22	2.73
S9	25.69	23.89	2.65	5.78
S10	25.95	24.67	3.32	5.55

Fig. 6 **a** Backscatter electron (BSE) image of sample B-1 showing stibnite grain (*right*) and surrounding secondary phases. Scorodite appears as a globular inclusion in another As–Sb–Fe phase. Location of the performed EDS line analysis is marked. **b** BSE image of decomposing stibnite grain showing the locations of EDS spot analyses performed (*S2–S8*). **c** BSE image of arsenian pyrite grain showing the locations od EDS spot analyses performed (S9, S10). **d** A series of EDS line analyses results for As, Fe, O, Sb, and S, expressed as wt%. **e** Table of EDS spot analyses results (*S1–S10*) indicating As, Fe, Sb and S wt% compositions

metre-scale in most of the battery site area, but was down to cm and even mm-scale within the secondary iron arsenates, and, in particular, the cemented scorodite-bearing hardpan material.

Other common metalloid sinks at the Big River processing site are presumed to be iron oxide/hydroxide phases. Even though XRD analyses of the mining substrates failed to identify the likely iron-rich phases present, the colour of the materials and the known presence of sulphide (iron-bearing) minerals in the mineralised rocks and in some of the mining residues, strongly suggest the presence of (possibly poorly crystalline) iron oxides or hydroxides. Iron compounds have long been known to be important scavengers of As as well as Sb and one of the most

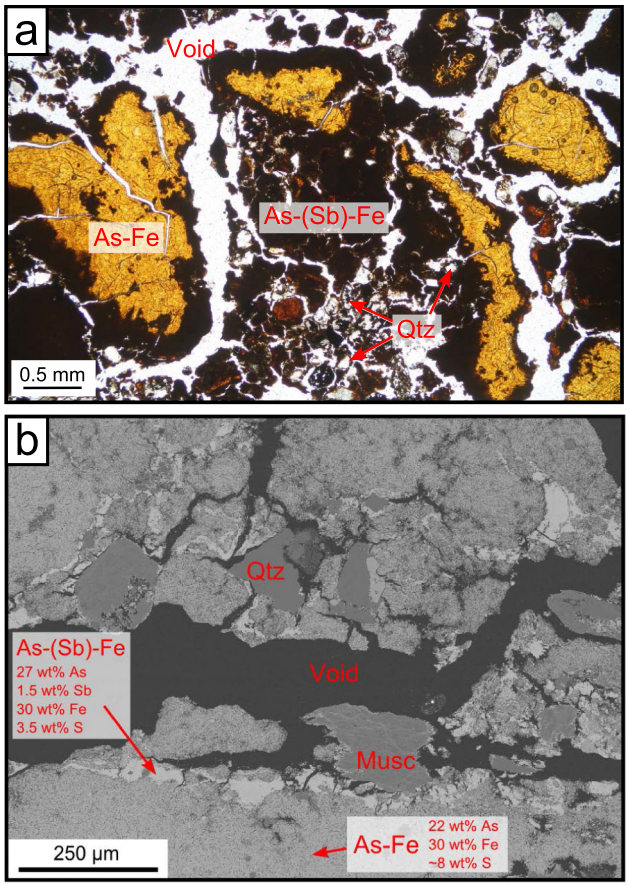

Fig. 7 Microphotographs of sample B-2 showing two distinctive As–(Sb)–Fe phases and subrounded quartz grains. **a** Microscope image under plane-polarised light (PPL). **b** Backscatter electron (BSE) image showing the results of the EDS analyses

common minerals found in historic gold mine settings in New Zealand is ferrihydrite combined with arsenate (Craw et al. 2004; Haffert et al. 2010; Wilson et al. 2004a). Poorly-crystalline phases, e.g. Fe(III) hydroxides such as two-line ferrihydrite, are known to have particularly high sorptive capacities (Bowell 1994; Fuller et al. 1993; Gal et al. 2007; Jain et al. 1999; Jambor and Dutrizac 1998; Pierce and Moore 1982; Waychunas et al. 1993). At other New Zealand mine sites, As concentrations were found to reach 20 wt% locally in these materials (Haffert et al. 2010). At the Big River processing site, the typical As content of the common brown-coloured residues ranges from <1 to ≈10 wt% (Table 1). The affinity of metalloids towards iron phases has been well documented in experimental (e.g. Álvarez-Ayuso et al. 2013; Jain et al. 1999; Mitsunobu et al. 2010; Waychunas et al. 1993) and field settings (e.g. Courtin-Nomade et al. 2003; Craw and Chappell 2000; Gal et al. 2007; Ritchie et al. 2013) and the mechanisms responsible for their association are mainly co-precipitation and adsorption. The latter is pH dependent. Arsenate species predominate under oxidising conditions in soils, mainly $H_2AsO_4^-$ and $HAsO_4^{2-}$; their adsorption onto iron oxide and hydroxide surfaces is favoured when the net charge of the mineral surfaces is positive. This occurs under specific pH conditions for different minerals, usually between 4 and 7 for iron oxides (Bowell 1994; Boyle and Jonasson 1973; Garcia-Sanchez and Alvarez-Ayuso 2003). Antimony also forms oxyanions, particularly SbO_3^-, in the natural environment and for this reason, adsorption of Sb with similar pH dependence to arsenic can be expected. Since the pH at the battery site oscillates around 2–3, the possibility of metalloid leaching from the site cannot be discounted, even though extremely high concentrations persist in association with iron oxide/hydroxide phases.

Yet another possible sink for both metalloids is adsorption onto clay mineral surfaces (Foster et al. 1998; Sadiq 1997). This is particularly true in acidic soils where positively charged clay particles exist and adsorption of As and Sb oxyanions is more likely (Sadiq 1997; Xi et al. 2010). According to Xi et al. (2010), the optimal pH for Sb(V) adsorption is 3.6, at which almost 75 % removal can occur. Given the presence of kaolinite in the Big River mine's processing residues (Table 1), this mechanism of As and Sb retention can also be expected.

The Big River battery site contains residues ranging from non-oxidised (sample B-4), through partially to fully oxidised. The formation of hardpan layers and precipitation of authigenic As and Sb-rich phases has largely immobilised the metalloids and isolated the primary sulphide minerals (arsenopyrite, pyrite, and stibnite) from the surficial environment, thereby preventing their further decomposition. The separation of the sulphide minerals, resulting in their preservation, represents a mechanism of As and Sb immobilisation and the minerals' survival is thought to have been possible thanks to two processes: (1) encapsulation by secondary phase formation (scorodite and As–(Sb)–Fe phases, as demonstrated in sample B-1), which isolated the minerals from direct contact with oxygen and water, and (2) burial in a saturated, reducing environment, as in the example of the grey-coloured sample B-4, which is thought to have been exposed by recent river bank erosion. The sulphide preservation in this setting agrees well with the findings of Craw et al. (2003) who demonstrated that arsenopyrite can be stable in a water-saturated near-surface environment. The now-exposed unsolidified material is expected to undergo gradual oxidation and secondary arsenic and iron-rich phases may also form.

Overall, apart from the indirect control by environmental conditions, the mobility of As and Sb in the studied residues is controlled by various crystalline and amorphous phases produced by the decomposition of primary minerals that were unstable in the surficial oxidised environment.

For the most part, the processing residues are expected to remain immobilised, as long as conditions persist that are favourable for the stability of secondary minerals and the adsorption of metalloids onto iron oxides/hydroxides and clays. A field-based study of arsenopyrite-rich mining residues in Manitoba, Canada demonstrated that destabilisation of secondary phases (in that case: jarosite, scorodite, and iron sulphoarsenates) is possible when local site conditions change (Salzsauler et al. 2005). In that case, capping of the mining residues resulted in the development of a reduced environment in the pile and subsequent leaching of the attenuated arsenic into groundwater (Salzsauler et al. 2005).

Water Quality

The impact of the mine site on water quality appears to be only local in its extent. Only small volumes of water drain the site as small creeks and visible seeps ($\approx$1 L/s combined, during dry weather). No As or Sb were detected in Big River downstream of the site due to immediate dilution with $\approx$50 L/s Big River waters. It is likely that noticeably higher metalloid fluxes are released into the Big River during times of prolonged wet weather when the site becomes saturated and more water has a chance to interact with the mining substrates for a prolonged time. Even then, however, the metalloid concentrations are expected to be significantly diluted immediately on confluence with the Big River.

Metalloid concentrations in smaller creeks and seeps were up to 0.85 mg/L for As and 0.007 mg/L Sb. A comparison with waters associated with other historic and active mines in New Zealand (Fig. 8) indicates that these results lie within the typical range documented for historic gold mining sites. The neutral character of water draining the waste rock pile is likely the result of carbonate minerals presence in the host rocks buffering any acidity generated from sulphide mineral decomposition. Neutral pH waters can contain elevated metalloid concentrations (e.g. at the Globe Progress and Endeavour Inlet mines, Fig. 8; Druzbicka and Craw 2013; Wilson et al. 2004b). Although local acidification of waters is possible at mining and processing sites (e.g. wetland at the Prohibition Mill site, pH $\approx$ 4; Haffert and Craw 2008a, b), in the case of the Big River site, the low pH recorded can be attributed to the presence of humic substances (humic and fulvic acids) in the Big River water and is not due to the generally low pH of the processing site's soils and mining residues. The humic substances content in Big River has not been measured but it is presumed to be relatively high, given the characteristic deeply orange-brown colour of the water both upstream and downstream of the mine site. The increased acid concentrations derive from decomposing organic matter in soil and swamps and are typical in the streams and rivers in the West Coast (e.g. Winterbourn and Collier 1987).

From an environmental hazard perspective, even though the dissolved metalloid concentrations in water at the Big River mine site exceed the environmental guideline values for protection of aquatic ecosystems of 0.001 mg/L for As and the provisional value of 0.009 mg/L for Sb (ANZECC 2000), the amount of water affected and the immediate natural remediation through dilution at the confluence with the Big River ensure that no serious environmental risks are posed.

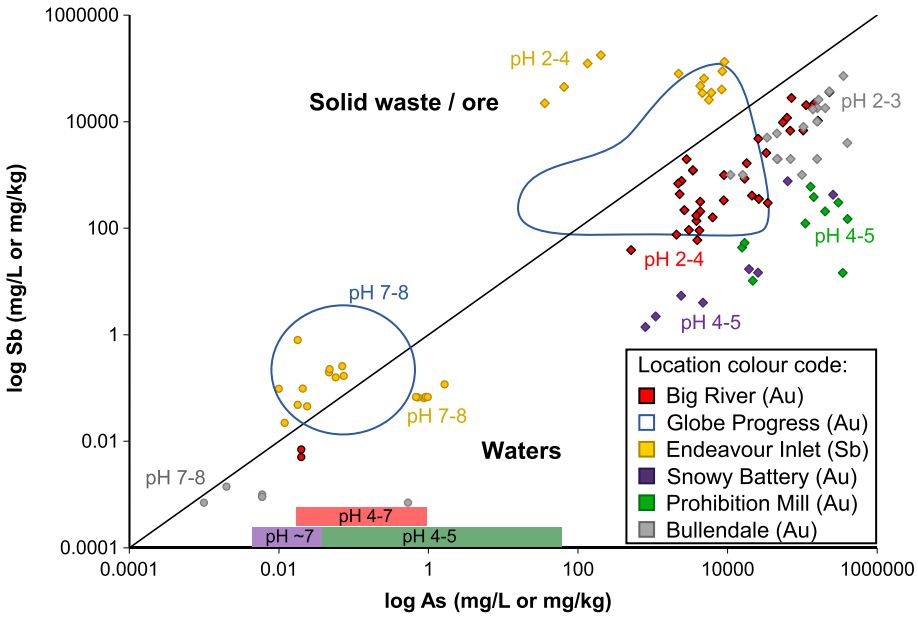

Fig. 8 Arsenic and antimony concentrations in solid wastes (and Globe Progress mine ore) and waters at mining sites in New Zealand. Water results for Big River, Snowy Battery and Prohibition Mill sites indicated with *coloured rectangles* represent the ranges of As concentrations recorded where Sb was undetectable. Data sourced from OceanaGold Ltd, Haffert and Craw (2008a, 2010), Wilson et al. (2004a, b)

Figure 8 presents metalloid concentrations of discharge waters relative to compositions of mining residues at the Big River processing site (red symbols in the top of the graph). Data from other historic mine sites in New Zealand are added for comparison. In most cases, i.e. at the Big River, Snowy Battery, Prohibition Mill, and Bullendale mining sites, As is the dominant metalloid present, and only waste materials at the Endeavour Inlet antimony smelter site contain Sb > As. The formation of secondary minerals in all of these mining residues play an important role in metalloid attenuation and localised acidification has been recognised as important in ensuring the stability of some of the phases present (Haffert and Craw 2008b, 2010; Wilson et al. 2004a, b).

Conclusions

The oxidation of arsenopyrite, arsenian pyrite, and stibnite at the Big River mine's processing site resulted in the development of extremely metalloid-rich mining residues (up to ≈ 25 wt% As and 3.6 wt% Sb) in the 70 years since the gold mine closed in 1942. Processing residues at the battery site have been oxidised to varying degrees and oxidation of sulphide minerals has resulted in the localised acidification of the substrates, typically to pH ≈ 3. Metalloid mobilisation has occurred on a metre, cm, and mm-scale at the processing site. Large quantities of As and Sb have been immobilised on site, most likely through a combination of processes, principally involving the formation of secondary As phases such as scorodite, amorphous iron arsenate, and iron sulphoarsenate. In addition, co-precipitation and/or adsorption onto iron oxides/hydroxides and adsorption onto clays likely also acted as local sinks for As and Sb.

The sustained low pH of the mining residues at the Big River mine's processing site contributes to the As and Sb attenuation by ensuring the survival of the secondary minerals, the solubility of which often increases with rising pH. In addition, the formation of secondary minerals is also responsible for the minimisation of metalloid mobility through isolation of the primary As and Sb minerals from the oxidised environment.

It is possible that parts of the site have already attained equilibrium through the natural restoration processes that have been taking place since the mine's closure in 1942. The immobilisation of As and Sb persists despite the wet climate, which is characterised by an annual rainfall of over 2,000 mm, which ensures generally high moisture levels and, in some places, waterlogged conditions year-round. Dissolved metalloid concentrations in the mine's waters reached 0.85 mg/L As and 0.007 mg/L Sb, and the pH of the mine drainage ranged from 3.8 to 7.3. The elevated metalloid concentrations are immediately diluted to undetectable levels as the water flows into the Big River.

Acknowledgments This study was funded by the NZ Ministry of Business, Innovation, and Employment and the University of Otago. The Department of Conservation kindly permitted sampling at the historic site. We are grateful to Dave Hodson for his assistance in the field and to OceanaGold Ltd for logistical support. Technical assistance from Kat Lilly and Damian Walls is appreciated. Helpful reviews by two anonymous referees and Dr. R. Kleinmann improved the manuscript.

References

Álvarez-Ayuso E, Otones V, Murciego A, García-Sánchez A (2013) Evaluation of different amendments to stabilize antimony in mining polluted soils. Chemosphere 90:2233–2239

ANZECC (2000) Australian and New Zealand guidelines for fresh and marine water quality. Australian and New Zealand Environment and Conservation Council and Agriculture and Resource Management Council of Australia and New Zealand

APHA (2005) Standard methods for the examination of water and wastewater, 21st edn. American Public Health Assoc, Washington DC

Ashley P, Lottermoser B (1999) Arsenic contamination at the Mole River mine, northern New South Wales. Aust J Earth Sci 46(6):861–874

Ashley P, Craw D, Graham B, Chappell D (2003) Environmental mobility of antimony around mesothermal stibnite deposits, New South Wales, Australia and southern New Zealand. J Geochem Explor 77(1):1–14

Barry J, Armstrong B (1993) The history and mineral resources of the Reefton goldfield. Resources Information Report 15, Energy and Resources Division, Ministry of Commerce, p 59

Blakemore L, Searle P, Daly B (1987) Methods for chemical analysis of soils. NZ Soil Bur Sci Rep 80:71–76

Bowell R (1994) Sorption of arsenic by iron oxides and oxyhydroxides in soils. Appl Geochem 9(3):279–286

Boyle R, Jonasson I (1973) The geochemistry of arsenic and its use as an indicator element in geochemical prospecting. J Geochem Explor 2(3):251–296

Christie A, Brathwaite R (2003) Hydrothermal alteration in metasedimentary rock-hosted orogenic gold deposits, Reefton goldfield, South Island, New Zealand. Miner Deposita 38(1):87–107

Christie A, Corner N, Bierlein F, Smith P, Ryan R, Arne D (2000) Disseminated gold in turbidite-hosted gold deposits of Reefton (South Island, New Zealand), Victoria (Australia) and Nova Scotia (Canada). In: Proceeding NZ Minerals and Mining Conference, Crown Minerals, Ministry of Economic Development, Wellington, New Zealand, pp 105–118

Christie A, Barker R, Brathwaite R (2010) Mineral resource assessment of the West Coast Region, New Zealand. GNS Science Report 2010/61, p 235

Cooper R (1974) Age of the Greenland and Waiuta Groups, South Island, New Zealand (Note). NZ J Geol Geophys 17(4):955–962

Courtin-Nomade A, Bril H, Neel C, Lenain J-F (2003) Arsenic in iron cements developed within tailings of a former metalliferous mine-Enguialès, Aveyron, France. Appl Geochem 18(3):395–408

Craw D, Chappell D (2000) Metal redistribution in historic mine wastes, Coromandel Peninsula, New Zealand. NZ J Geol Geophys 43(2):187–198

Craw D, Falconer D, Youngson J (2003) Environmental arsenopyrite stability and dissolution: theory, experiment, and field observations. Chem Geol 199(1):71–82

Craw D, Wilson N, Ashley P (2004) Geochemical controls on the environmental mobility of Sb and As at mesothermal antimony and gold deposits. Appl Earth Sci 113(1):3–10

DeSisto S, Jamieson H, Parsons M (2011) Influence of hardpan layers on arsenic mobility in historical gold mine tailings. Appl Geochem 26(12):2004–2018

Druzbicka J, Craw D (2013) Evolving metalloid signatures in waters draining from a mined orogenic gold deposit, New Zealand. Appl Geochem 31:251–264

Filippi M, Machovič V, Drahota P, Böhmová V (2009) Raman microspectroscopy as a valuable additional method to X-ray diffraction and electron microscope/microprobe analysis in the study of iron arsenates in environmental samples. Appl Spectrosc 63(6):621–626

Foster A, Brown G Jr, Tingle T, Parks G (1998) Quantitative arsenic speciation in mine tailings using X-ray absorption spectroscopy. Am Mineral 83(5):553–568

Frau F, Ardau C (2004) Mineralogical controls on arsenic mobility in the Baccu Locci stream catchment (Sardinia, Italy) affected by past mining. Mineral Mag 68(1):15–30

Fuller C, Davis J, Waychunas G (1993) Surface chemistry of ferrihydrite: part 2. Kinetics of arsenate adsorption and coprecipitation. Geochim Cosmochim Acta 57(10):2271–2282

Gage M (1948) The geology of the Reefton quartz lodes. NZ Geol Survey Bull 42, Wellington, New Zealand

Gal J, Hursthouse A, Cuthbert S (2007) Bioavailability of arsenic and antimony in soils from an abandoned mining area, Glendinning (SW Scotland). J Environ Sci Health A 42(9):1263–1274

Garcia-Sanchez A, Alvarez-Ayuso E (2003) Arsenic in soils and waters and its relation to geology and mining activities (Salamanca Province, Spain). J Geochem Explor 80(1):69–79

Gieré R, Sidenko N, Lazareva E (2003) The role of secondary minerals in controlling the migration of arsenic and metals from high-sulfide wastes (Berikul gold mine, Siberia). Appl Geochem 18(9):1347–1359

Groves D, Goldfarb R, Gebre-Mariam M, Hagemann S, Robert F (1998) Orogenic gold deposits: a proposed classification in the context of their crustal distribution and relationship to other gold deposit types. Ore Geol Rev 13(1):7–27

Haffert L, Craw D (2008a) Mineralogical controls on environmental mobility of arsenic from historic mine processing residues, New Zealand. Appl Geochem 23(6):1467–1483

Haffert L, Craw D (2008b) Processes of attenuation of dissolved arsenic downstream from historic gold mine sites, New Zealand. Sci Total Environ 405(1):286–300

Haffert L, Craw D (2009) Field quantification and characterisation of extreme arsenic concentrations at a historic mine processing site, Waiuta, New Zealand. NZ J Geol Geophys 52(3):261–272

Haffert L, Craw D (2010) Geochemical processes influencing arsenic mobility at Bullendale historic gold mine, Otago, New Zealand. NZ J Geol Geophys 53(2–3):129–142

Haffert L, Craw D, Pope J (2006) Quantification and controls on As distribution in Westland, New Zealand. In: Proceeding, 39th AusIMM New Zealand Branch Annual Conference. http://www.crl.co.nz/downloads/geology/Haffert-%20AusIMM%202006.pdf

Haffert L, Craw D, Pope J (2010) Climatic and compositional controls on secondary arsenic mineral formation in high-arsenic mine wastes, South Island, New Zealand. NZ J Geol Geophys 53(2–3):91–101

Henderson J (1917) The geology and mineral resources of the Reefton Subdivision, Westport and North Westland Division. NZ Geol Survey Bull 18, Wellington, New Zealand

Hewlett L, Craw D, Black A (2005) Comparison of arsenic and trace metal contents of discharges from adjacent coal and gold mines, Reefton, New Zealand. Mar Freshwater Res 56(7):983–995

Jain A, Raven K, Loeppert R (1999) Arsenite and arsenate adsorption on ferrihydrite: surface charge reduction and net OH-release stoichiometry. Environ Sci Technol 33(8):1179–1184

Jambor J, Dutrizac J (1998) Occurrence and constitution of natural and synthetic ferrihydrite, a widespread iron oxyhydroxide. Chem Rev 98(7):2549–2586

Krause E, Ettel V (1989) Solubilities and stabilities of ferric arsenate compounds. Hydrometallurgy 22(3):311–337

Laird M, Shelley D (1974) Sedimentation and early tectonic history of the Greenland Group, Reefton, New Zealand. NZ J Geol Geophys 17(4):839–854

Langmuir D, Mahoney J, Rowson J (2006) Solubility products of amorphous ferric arsenate and crystalline scorodite ($FeAsO_4$·$2H_2O$) and their application to arsenic behavior in buried mine tailings. Geochim Cosmochim Acta 70(12):2942–2956

Lottermoser BG (2010) Mine wastes: characterization, treatment and environmental impacts. Springer, Berlin, Germany

Milham L, Craw D (2009) Two-stage structural development of a Paleozoic auriferous shear zone at the Globe-Progress deposit, Reefton, New Zealand. NZ J Geol Geophys 52(3):247–259

Mitsunobu S, Takahashi Y, Terada Y, Sakata M (2010) Antimony (V) incorporation into synthetic ferrihydrite, goethite, and natural iron oxyhydroxides. Environ Sci Technol 44(10):3712–3718

Pierce M, Moore C (1982) Adsorption of arsenite and arsenate on amorphous iron hydroxide. Water Res 16(7):1247–1253

Ritchie V, Ilgen A, Mueller S, Trainor T, Goldfarb R (2013) Mobility and chemical fate of antimony and arsenic in historic mining environments of the Kantishna Hills district, Denali National Park and Preserve, Alaska. Chem Geol 335:172–188

Sadiq M (1997) Arsenic chemistry in soils: an overview of thermodynamic predictions and field observations. Water Air Soil Pollut 93(1–4):117–136

Salzsauler K, Sidenko N, Sherriff B (2005) Arsenic mobility in alteration products of sulfide-rich, arsenopyrite-bearing mine wastes, Snow Lake, Manitoba, Canada. Appl Geochem 20(12):2303–2314

Tulloch A (1983) Granitoid rocks of New Zealand-a brief review. Geol Soc Am Mem 159:5–20

US-EPA (2007) Field portable X-ray fluorescence spectrometry for the determination of elemental concentrations in soil and sediment. US-EPA Method 6200, US Environmental Protection Agency, Washington DC

Waychunas G, Rea B, Fuller C, Davis J (1993) Surface chemistry of ferrihydrite: part 1. EXAFS studies of the geometry of coprecipitated and adsorbed arsenate. Geochim Cosmochim Acta 57(10):2251–2269

Wilson N, Craw D, Hunter K (2004a) Antimony distribution and environmental mobility at an historic antimony smelter site, New Zealand. Environ Pollut 129(2):257–266

Wilson N, Craw D, Hunter K (2004b) Contributions of discharges from a historic antimony mine to metalloid content of river waters, Marlborough, New Zealand. J Geochem Explor 84(3):127–139

Winterbourn M, Collier K (1987) Distribution of benthic invertebrates in acid, brown water streams in the South Island of New Zealand. Hydrobiologia 153(3):277–286

Wright L (1993) Big River quartz mine 1882–1942: a worthwhile speculation. Friends of Waiuta Inc, Reefton

Xi J, He M, Lin C (2010) Adsorption of antimony (V) on kaolinite as a function of pH, ionic strength and humic acid. Environ Earth Sci 60(4):715–722